RESEARCH ARTICLE

Development of an IoT-based MANET for Healthcare Monitoring System Using Data Loss Aware Routing Protocol

K. Balasubramanian[1] · S. Senthilkumar[2] · N. Kopperundevi[3] · S. Sivakumar[4]

Received: 3 December 2024 / Revised: 20 May 2025 / Accepted: 10 June 2025

Abstract

Healthcare needs a major shift to more measurable and affordable solutions. The answer to these challenges is to focus on restructuring the healthcare system to prevent illness, not illness, and on disease prevention and early detection. The Internet of Things (IoT) communicates with mobile ad hoc networks (MANETs) in a smart environment, making it more attractive and cost-effective for consumers. Recently, MANET-IoT systems have been used in many areas of live applications. In addition, most routing protocols are for MANET, but they are not compatible with MANET-IoT. However, one of the key apparatuses of the MANET-IoT system is the loss of records due to unreliable routing. In this article, we suggest an optimal cluster founded data loss aware routing protocol, MANET-IoT, for healthcare monitoring systems (OCDL-HM). First, we introduce efficient cluster formation using the butterfly-induced sunflower optimization (BSFO) algorithm, which enhances the energy efficiency of routing. Then, the cluster head (CH) of every cluster is computed through a cuckoo search based deep probability neural network (CS-DPNN) with different design metrics. The CH node is acting as an intermediate node between cluster members and the next neighbouring CH node. After that, the next neighbouring CH node is selected by a hybrid recurrent dynamic neural network (RDNN), which provides data lossless routing between nodes. Finally, the simulation results of proposed and existing routing protocols analyzed with different simulation scenarios in terms of energy consumption, packet loss ratio, network lifetime, number of active nodes, packet delivery ratio, throughput, and latency.

Keywords Healthcare monitoring · MANET-IoT · Cluster formation · CH selection · Routing

Abbreviations

IoT	Internet of Things
MANET	Mobile ad hoc networks
OCDL-HM	MANET-IoT, for healthcare monitoring systems
BSFO	Butterfly-induced sunflower optimization
CH	Cluster head
CS-DPNN	Cuckoo search based deep probability neural network
RDNN	Recurrent dynamic neural network
AQRouting	Adaptive routing protocol
NS-3	Network Simulator-3
SNR	Signal-to-noise ratio

 https://doi.org/10.1007/s44196-025-00896-3

Published online: 20 August 2025

 https://doi.org/10.1007/s44196-025-00896-3

DCNI	Dynamic critical node identification
DISNEY	Distinct Network Yarning
AODV	Ad hoc On-Demand Distance Vector
ORGMA	Opportunistic routing protocol
A-EEBLR	Ant-based efficient energy and balanced load routing technique
DSDV	Destination-Sequenced Distance-Vector Routing
OLSR	Optimized Link State Routing Protocol
DMRP	Dynamic Mobile Routing Protocol
SAR	Self-adaptive and reliable protocol
SEAL	Software Encryption Algorithm
GPSR	General Packet Radio Service
BOA	Butterfly optimisation algorithm

1 Introduction

By integrating the virtual and physical worlds, IoT builds an integrated communication framework for interconnected communities and operating systems. With the advent of digital remote care IoT systems, editing medical records has become more common. Health is one of the most popular IoT applications, trying to monitor patients' major symptoms on a weekly basis and eliminate the need for hospitalization. A number of devices have been connected in the healthcare system to accumulate patient material, including environmental nursing sensors and patient-sensitive and non-structured news devices. Technology is already at the highest level, and we need to accelerate the process of meeting people and their needs in a technology project. It is essential to effectively reflect the changes that occur [1]. Flexible sensors in dynamic surroundings are surrounded by the MANET-IoT, which transmits environmental data to nursing homes for use in healthcare applications. Because IoT networks are wireless, secure data transfer is important in a healthy environment. Integrating the Internet of Things (IoT) with Mobile Ad Hoc Networks (MANETs) offers several distinct advantages for healthcare applications, particularly in dynamic and resource-constrained environments. Firstly, this integration facilitates real-time, decentralized, and infrastructure-independent communication among heterogeneous medical devices, enabling continuous patient monitoring even in remote or mobile settings. IoT devices, such as wearable sensors and medical implants, can gather critical physiological data, while MANETs allow these devices to form self-configuring networks that dynamically adapt to changes in topology, ensuring reliable data transmission without the need for fixed infrastructure. This is especially beneficial in emergency scenarios, rural healthcare delivery, and disaster response, where centralized communication systems may be unavailable. Furthermore, combining MANETs with IoT enhances scalability and fault tolerance, allowing the healthcare monitoring network to remain operational even when individual nodes fail or move. The integration also supports efficient resource utilization, as MANET protocols can optimize routing paths based on energy constraints and node availability. Overall, the synergy between IoT and MANET strengthens the robustness, adaptability, and responsiveness of healthcare systems, paving the way for intelligent, patient-centric, and continuous care delivery models.

There are several reasons why data gathered from sensors integrated into medical equipment could be lost during the transfer process. Therefore, it is important to establish a path for free data communication on MANET-IoT networks in the context of healthcare. Moreover, as technology becomes more important in all areas of life, we are more susceptible to risks such as safety spells and the resulting delays. Opportunely, we now have the ability to detect and eradicate security threats on smaller networks. Though, for larger networks, existing security events may be less reliable [2]. The latest submissions used on smart devices involve more computing power and more memory volume [3]. Smart health care systems have recently evolved in a rapid manner [4]. Not all such requests can be secured by single cloud server. Communication between MANET and IOT opens up new avenues for complex issues related to service delivery and its network features in a smart environment. One of

the major problems with MANET-IOT schemes is the functionality of the network nodes: algorithm design the routing protocol necessity be effective for terrain changes [5–7]. In mobile ad hoc networks (MANETs), terrain changes—such as moving from an open field to a dense urban environment—can significantly impact routing protocols by altering signal propagation and connectivity between nodes. For example, in a healthcare emergency response scenario, mobile IoT-equipped ambulances moving through hilly or forested terrain may experience signal attenuation or blockage due to physical obstructions. This can cause frequent link breaks, increased packet loss, and higher latency, making it difficult for traditional routing protocols to maintain stable paths. As a result, routing protocols must be adaptive and robust enough to handle such dynamic topological changes to ensure reliable data transmission, especially when transmitting critical patient information. We designate the enterprise and implementation of AQ-Routing and analyze its concert using simulations and metrics founded on our application. The adaptive routing protocol (AQRouting) Learning Enhancement methods can control the amount of traffic at different times so that the routing metric can be updated for each node [8–10].

Internet of Things (IoT) is a powerful link between the digital and physical worlds and is part of a changing Internet model. Its compatibility with smart objects and global communication is a key integration concept of IoT systems. In all kinds of objects, such as smart phones, sensors, or devices, are part of the Internet, interacting with interacting networked objects (such as RFID) [11, 12]. IoT is widely used in many areas, including medical care, home automation, industrial automation, mobile healthcare, power transmission, and distribution [13]. Components include understanding, data recovery, multivariate linking, and data processing.

MANETs [14, 15] are emerging as major technologies that integrate the routing function into mobile nodes to enhance the robust and effective operation of mobile wireless networks. These networks are wireless links that regulate relative bandwidth; they are regarded as random and multi-hop topologies, and they can change dynamically and sometimes quickly [16–18]. In such settings you can find various options to connect the IoT device to the MANET terminal. IoT expedients over an Internet-fixed MANET require several terrains of the MANET [19]. Cluster topology refers to the controller MANET nodes for IoT devices or associated IoT procedures. Routing for IoT Nodes on MANETs MANET routing protocols use IoT devices connected to MANET nodes.

Low power LASI networks, abbreviated as LLN [20], are networks with a fixed number of routers that are unlikely to communicate with each other. The routing protocol for Low Power and Loss Networks was proposed by the IETF Working Collection for the development of LLNs based on 6LoWPAN. Power and Loss Networks is a remote vector routing protocol designed for low power LASI networks using IPV6 principles [21]. Developing effective routing protocols on a MANET is always difficult due to the above features [22, 23]. An effective routing protocol must be able to adapt properly to these topographic variations, and the control information in the protocol must be kept to a minimum due to bandwidth control. A wide range of temporary routing protocols have been suggested, in terms of evaluating network environment. To cope with the changing environment, some routing models try to adapt to the network context, varying in time and place [24].

2 Problem Statement

Serhani et al. [1] have proposed a routing protocol (AQ-routing) is based on enhanced learning aimed specifically at raising awareness of node mobility and connection stability. A motion uncovering model was planned that would consent every node to be matched to a new metric baptized the Q-metric based on the updated motion aspect. Therefore, each network node can change its routing behaviours depending on the network situations around it, and AQ-routing can progress connection steadiness in static and portable environments and growth pocket delivery speed related to existing routing facsimiles. The IoT field is growing, mainly due to its various achievements in the diagnosis, prevention, and diagnosis of various infections [29, 32] in patients.

At the heart of this new technology is the need to further explore IoT security risks, as IoT is widely used to obtain information from the environment for a more user-friendly user experience [34]. In general, IoT integrates with MANET in a better environment, making it more desirable and less expensive. MANET-IoT can be used

not only for tragedy states but also for robotic message. At the same time, networking activities open up new complex issues. At MANET-IoT, energy consumption and traffic management are key issues in managing health information [25–27, 35]. Information such as the location of events needs to be sent or forwarded for quick and accurate response. However, it can be difficult to pass this information on to a medical canter or specialist. In these situations, the transfer of opportunistic knowledge plays an important role [32, 33]. Current routing protocols require large notices of cluster overload, which can lead to high power consumption and pocket loss. There are several modern routing models available based on reliable measurements to improve MANET-IoT data loss [34]. However, there are still many challenges in ensuring an effective data loss awareness environment due to the dynamic nature of the network.

Our contributions: An optimal cluster-based data loss aware routing protocol MANET-IoT is proposed for healthcare monitoring system (OCDL-HM). The main contributions of proposed OCDL-HM routing protocol are summarized as follows:

1. A cluster formation is done using butterfly induced sunflower optimization (BSFO) algorithm which enhances energy efficiency of routing.
2. CH of each cluster is computed through cuckoo search based deep probability neural network (CS-DPNN) with the different design metrics.
3. The next neighbouring CH node is select by hybrid recurrent dynamic neural network (RDNN) which provides data lossless routing between nodes. In conclusion, various modelling scenarios were used to analyse the simulation results of both proposed and current routing protocols with respect to energy consumption, the number of active nodes, network lifetime, packet delivery ratio, packet loss ratio, throughput, and delay.

The remainder of the paper is structured as follows in advance: Section 2 talks about the latest research on MANET and IoT routing technologies. The suggested routing protocol's network model and problem methodology are covered in Sect. 3. Section 4 provides a full functional description of the proposed OCDL-HM routing protocol. Subsequently, Sect. 5 presents the simulation results and a comparison study of the suggested and current routing protocols. In Sect. 6, the paper finally comes to an end.

3 Related Works

Kang et al. [25] have proposed evaluation of routing algorithms using Network Simulator-3 (NS-3) simulations to detect major vulnerabilities and evaluate their performance. We are creating ORGMA, a dependable and user-friendly opportunistic routing technology for MANETs, based on our observations. Our method, known as gradient sharing, alters the sender's packet and prevents the receivers from routing. Our contribution includes the use of immediate signal-to-noise ratio (SNR) to improve cost-effective management in terms of routing and flood costs. They allow ORGMA to achieve high pocket delivery rates in dynamic MANET environments.

Karmel et al. [26] have proposed a hop node is selected based on measurements such as the A-EEBLR approach, delay, power throughput, high load and connection quality. The likelihood of choosing the subsequent hop node to be an adjacent node is calculated using these measurements. The likelihood of the upcoming hop is that multiple paths will be placed by the ants and their pin agents, from which the best transfer path will be chosen. Empirical findings indicate that the A-EEBLR technique outperforms the existing A-ESR technique in terms of packet count, node count, and node movement.

Bento et al. [27] have proposed a HyphaNet offers a new bio-inspired approach to fungal dynamics that paves the way for creating, improving and selecting paths for MANETs. The paths in the HyphaNet, are built like a mushroom mycelium, with many parallel paths actually installed, but over time only the paths of the improved paths will come alive to strengthen and thicken their walls, ensuring debris and greater flow attraction. In this new algorithm, the routing process follows the concept of attraction, in which data flows through areas of high density

of inactive organisms, i.e., low cost and high resource availability. A lightweight and safe routing programme with several routing and trust management features that can adjust to various IoT environment scenarios has been proposed by Hammi et al. [28]. For the purpose of analysis and assessment, we suggest using a probability model that considers both traffic and non-traffic behaviour events, which have an impact on a node's routing performance. We evaluated the effectiveness of our suggested routing method against SMORT and DMRP, two other general-purpose routing algorithms, using this mathematical model as a basis.

Garg et al. [29, 30] have proposed a developing Smart Architecture Considers the Author for Pocket Routing. These packages should be sent in the best possible manner in the presence of IoT. The routing protocol describes what communications take place on the routers. The computer sends information to determine the path between two network nodes. The router already knows what kinds of networks are connected. On the other hand, several studies have been conducted to determine the impact of black hole attack on the Ad hoc On-Demand Distance Vector (AODV) based network. A mathematical modelling study that satisfies the requirements of MRTS stability, optimisation, and loop fragmentation has been provided by Djedjig et al. [31]. It demonstrates that the particular trust-based routing metric possesses the tonicity and monotonicity qualities needed by the routing protocol.

MRTS is a strategy that described using ideas from game theory for repetitive confusion in prisoners and demonstrate the features of its joint implementation. Mathematical analysis and the results of evolution simulation clearly show that MRTS is an active approach to improving the stability and evolution of the IOT. Niu et al. [32] have proposed a dynamic critical node identification (DCNI). Initially, we suggest an all-encompassing metric to assess a node's importance inside a geographic picture. We then provide a sliding temporal window to link key values of the same node to several topographic snapshots and filter spatial snapshots that are closely related to the present snapshot. Ultimately, the outcomes of the joint focus ranking are used to choose the critical nodes. Then, at crucial nodes, the port jump mechanism can be employed to improve network security capabilities. An SDN-controlled MANET-based Open flow Switch screen that offers effective security threading has been proposed by Maruthupandi et al. [33]. By streamlining the path and saving time and effort, SDN is crucial to MANET management. For SDN-controlled MANETs, the Distinct Network Yarning (DISNEY) routing protocol prevents overloaded communications over MANET routing. The root fabric processing table maintains effective routing to reduce performance deterioration. You can choose the finest and safest route with the aid of this routing plan. Table 1 represents the summary of the research gap.

Simpson et al. [34] have proposed the help of edge computing it has created a vaguely based trust environment to reduce security threats in smart cities. A credible setting safeguards timely detection of malicious companies and detection of cooperative attacks. In edge computing, the calculations required to create the final tools are stored on the edge servers. This will decrease the idle time and bandwidth usage obligatory for traditional cloud admittance. Secure Seal uses an ambiguity-based method to prevent and isolate malicious nodes in the IoT network. Suspicious nodes are reviewed and re-analyzed based on the feedback value gained from the trust rating.

Chen et al. [35] have proposed the difficult of data gaining problem in the integrated switch scheme of the traditional control system. Due to the petit e-communiqué time and the high rate of pocket loss between vehicles, vehicles incoming the trunk lines are not able to transmit material on a regular basis through the integrated luggage control system. To solve this unruly, the specific protocol provides a live data transmission routing plan with the movement of trunk lines and the nearby street network. It addresses the difficult of data mobbing caused by high traffic on major roads, the problem of increasing segment information flow and packet loss, and the problem of link sharing caused by the lack of traffic that drives vehicles to move and exchange information.

4 Proposed Methodology

The proposed OCDL-HM routing protocol consists of set of process are cluster formation, CH selection and routing which can used to collect healthcare data from the patient to the healthcare system. The network model of anticipated OCDL-HM routing protocol is exposed in Fig. 1. First the healthcare information's have been

 https://doi.org/10.1007/s44196-025-00896-3

Table 1 Summary of Research Gap

Ref	Protocols	Methodology	Parameters	Remarks
21	ORGMA	Gradient forwarding approach	Accuracy	Increase data packet delivery speed to suit routing needs in this application script
22	A-EEBLR	Multi-controlled QoS energy conservation route based on improved ant colony	Number of Nodes	Achieves performance close to the best routing plan with global information
23	DSDV and OLSR	HyphaNet implements a process for plummeting RREQUEST circulation accessible in the poetry	Energy consumption	When calculating the number of pockets, the number of bundles, and the movement of the bundle
24	DMRP	Establishing trust between neighbouring devices	Network size	The more attractive the paths, the more likely you are to choose the holistic route
25	AODV	Definite paths are selected through routing methods	Node count	It is highly scalable compared to related jobs, our performance shows that it is efficient and excellent; it is also more suitable for larger and less secure IoT networks
26	ERNT	Trust management and calculation for IoT	Number of nodes	The pocket transfer speed was compared between the expected design and the previous design
27	SAR	Dynamic critical node identification	Mobility support	An Effective Approach to Improving the Sustainability and Development of the Internet of Things Network
28	DISNEY	Encryption and isolation	precision	A port jump mechanism can significantly improve network security by avoiding service attacks
29	SEAL	To examines the trust relations among the end users	Network size	Compared to the proposed method, the pocket transfer delay achieves the optimal ratio of performance and data transfer speed
30	GPSR	Traditional trunk line coordinated control method	Accuracy	The effectiveness of the planned action to reduce the impact of cooperative attacks is relatively high

gathered from the patient and OCDL-HM routing protocol is responsible to forward gathered data to the healthcare system. Finally, the patient data are analyzed by data analyzer and emergency alert can be given by the specialist doctor consultant.

In the proposed OCDL-HM routing protocol, first we explain the cluster formation using butterfly induced sunflower optimization (BSFO) algorithm. In second phase of this chapter, CH selection using CS-DPNN is presented. After that, we describe the next neighbouring node selection for routing which enables data lossless transfer from patient to the healthcare system. The authors Arora and Singh introduced the BSFO in 2018 [36]. The BSFO has gained widespread recognition for its powerful search skills and ability to accurately converge towards the global maximum point. BSFO offers good optimisation performance, is easy to implement, and can be easily adapted to any optimisation situation [37]. It has been widely employed in different fields in a short period, such as parameter identification, feature selection, data categorisation, and drought forecasting [38–44].

5 Cluster Formation Using Butterfly Induced Sunflower Optimization (BSFO) Algorithm

Cluster formation in MANET-IoT is used to change the configuration of mobile nodes to overcome various obstacles to network access. High energy efficiency, bandwidth reuse, goal tracking, data collecting, and network longevity are the primary objectives of clustering techniques. Lastly, clustering is a significant routing mechanism that saves energy. A cover hole may form for a number of reasons. The most recent adaptation method, known as the butterfly optimisation algorithm (BOA), mimics how butterflies behave as they feed and mate. The BOA technology is a

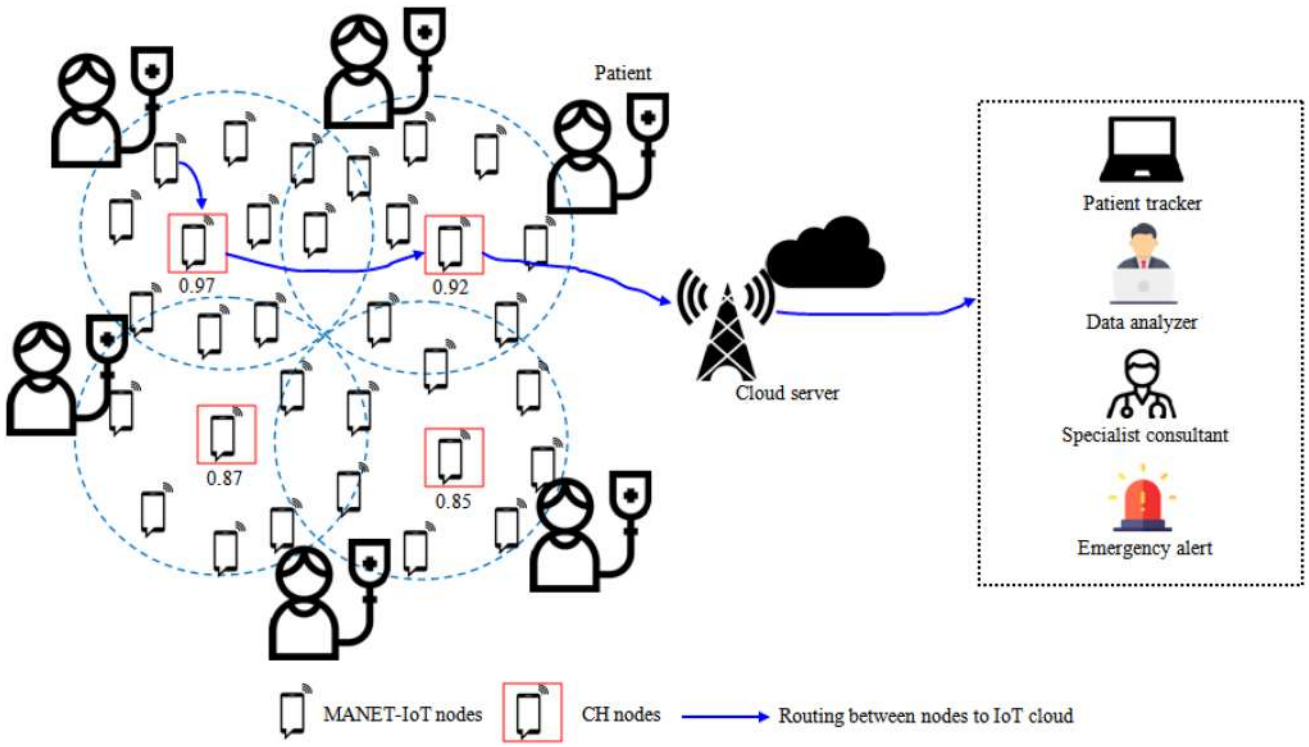

Fig. 1 Network model of proposed OCDL-HM routing protocol

meta-heuristic optimisation technique that emulates the processes of nectar seeking and natural cross-breeding. In the BOA, butterflies provide a unique flavour. The objective action of the solution, which is computed as follows in Eq. 1, is associated with this model:

$$g_j = d \times J^b \tag{1}$$

where g_j characterizes the perfume, j represents the stimulus strength, d and b represent the continuous. The iterative phase has two phases. Created a mathematical terminology for the global search phases formulated in Eq. 2:

$$y_j(s+1) = y_j(s) + (R^2 \times h^* - y_j(s)) \times g_j \tag{2}$$

where y_j indicates the location of jth butterfly, t represents the recurrence quantity, $R \in [0,1][0,1]$ is the random number, h^* represents the global optima, and g_j characterises the fragrance. Generating a local exploration grid is described as follows in Eq. 3:

$$y_j(s+1) = y_j(s) + (R^2 \times y_j(s) - y_K(s)) \times g_j \tag{3}$$

where y_j and y_K are i^{th} and K^{th} butterflies from the inhabitants. The overhead specified Eqs. (2) and (3) are achieved in BOA as given in Eq. 4:

$$\begin{cases} y_j(s+1) = y_j(s) + (R^2 \times h^* - y_j(s)) \times g_j & ifrand < q \\ y_j(s+1) = y_j(s) + (R^2 \times y_j(s) - y_K(s)) \times g_j & otherwise \end{cases} \tag{4}$$

where $q \in [0,1]$ is continual number. The worth of d is rationalized by the subsequent Eq. 5:

 https://doi.org/10.1007/s44196-025-00896-3

$$d(s+1) = d(s) + 0.025/(d(s) \times \max Iter \tag{5}$$

where $\max_{iter}$ represents the highest number of recurrences.

To maximise clustering design metrics, or butterfly induced sunflower optimisation (BSFO), the sunflower optimisation (SO) algorithm can be fused with the butterfly optimisation algorithm (BOA) to optimise the clustering parameters. One of the most recent advancements in soft computing techniques inspired by nature is BSFO. The basic idea of BSFO is to move in a manner similar to that of sunflowers, attempting to chase the sun after them. Every night, they go in the opposite way and wait for the sun to rise before setting out once more. The sunflower's sequence is achieved by the law of fallout as follows in Eq. 6:

$$P_Y = \frac{Q_Y}{4\pi R_Y^2} \tag{6}$$

where Q_Y represents the heat intensity (Y) customary by each sunflower; P_Y is the energy form solar and R_Y length between the finest person in the present populace and every person. Equation (7) displays the inverse rectangular association between the heat and space of the radiation. All sunflower reveals the direction toward the sun (2).

$$\vec{P}_Y = \frac{Y^* - Y_Y}{\left\|Y^* - Y_Y\right\|}, \quad Y = 1, 2, ...np \tag{7}$$

Y_y denotes each solution, where np is the population-specific size and Y* represents the best individual inside the current population. The following Eq. 8 describes a sunflower moving in the sun.

$$c_y = \lambda.Q_Y\left(\left\|Y_Y + Y_{Y-1}\right\|\right), \left\|Y_Y + Y_{Y-1}\right\| \tag{8}$$

where, λ is a certain constant connected to each sunflower's passive motion; $Q_Y(\left\|Y_Y + Y_{Y-1}\right\|$ is the sunflower is likely to crumble. The sunflower is thus pollinated to a new degree, where it moves in tiny circles around the sun, in contrast to other sunflowers that often move in favour of local search development. The mechanism for updating every sunflower circumstance is implemented through movement, based on the upstairs c_Y of the sunflower and their positioning t_Y towards the sun:

$$Y_{Y+1} = Y_Y + c_Y \times t_Y \tag{9}$$

When it comes to the two parameters that are defined—pollination rate (QR) and mortality (L)—SOA is actually subtle. Being highly compassionate does not make one capable of identifying the finest sunflower. Furthermore, every sunflower has a unique passive motion that governs the SOA search behaviour. Research investigations on SOA are not supported by any of these two restrictions. This article offers two solutions to get around the aforementioned restrictions. The pollination rate (QR) as mentioned in Eq. 10 should be changed from the standard stated value to the adaptive value (5) as the first modification.

$$QR = 0.5 \times \left(1 - \frac{z}{\max_z}\right) \tag{10}$$

This reckoning defines the co-efficient vector (QR) reduced linearly from 0.5 to 0 iterations. The second adjustment describes the passive displacement (λ) of each change of every sunflower as in Eq. 11.

$$\lambda = (V_a - M_a) \times \left(1 - \frac{z}{\max_z}\right) \tag{11}$$

where, V_a and M_a are the higher and inferior limits of the conclusion variables; z is the present repetition. Algorithm 1 describes the working function of the cluster formation using BSFO algorithm.

Algorithm 1 Cluster formation using BSFO algorithm

Input	: R_Y , g_j , P_Y
Output	: M_a , V_a
1	Produce initial populace of M butterflies
2	Prepare limits d, b, and q
3	While discontinuing standards not met do
4	Calculate terminology $y_j(s+1) = y_j(s) + (R^2 \times h^* - y_j(s)) \times g_j$
5	End for
6	Find the sunflower heat intensity $P_Y = \frac{Q_Y}{4\pi R_Y^2}$
7	if rand < q then
8	Update position using pollination rate $QR = 0.5 \times \left(1 - \frac{z}{\max_z}\right)$
9	Update the value of displacement (λ) using $\lambda = (V_a - M_a) \times \left(1 - \frac{z}{\max_z}\right)$
10	End while
11	Output the best solution for cluster formation

6 CH Selection Using Cuckoo Search Based Deep Probability Neural Network (CS-DPNN)

After cluster formation, we need to calculate the cluster head (CH) using the following design parameters which gathered from the mobile nodes such as energy consumption, mobility, conventional signal asset and congestion rate. The Cuckoo Search-based Deep Probability Neural Network (CS-DPNN) was chosen over other optimization techniques due to its superior ability to balance global exploration with local exploitation, which is critical for cluster head (CH) selection in dynamic and resource-constrained MANET-IoT environments. Traditional optimization algorithms such as Genetic Algorithms (GA) or Particle Swarm Optimization (PSO) often suffer from premature convergence or require extensive parameter tuning, which can limit their adaptability in highly mobile network conditions. In contrast, the Cuckoo Search (CS) algorithm, inspired by the brood parasitism of cuckoo birds, uses Lévy flight-based random walks to efficiently explore the search space, reducing the chances of getting trapped in local minima. When combined with the probabilistic reasoning and layered feature representation capabilities of a Deep Probability Neural Network (DPNN), the CS-DPNN framework offers a robust mechanism for selecting optimal CHs based on multiple criteria such as residual energy, signal strength, congestion, and mobility. This hybrid approach ensures more reliable and energy-efficient data aggregation and transmission, directly contributing to improved network stability and reduced packet loss in healthcare monitoring applications.

The cuckoo search (CS) algorithm is populace based stochastic global examination algorithm. This algorithm uses two different areas and updating the population throughout the process. In opinion, the main goal is to create improved cages based on the value of fitness rather than bad cages. As we all know, the first part of the standard Google search algorithm runs randomly about the best nest of current group and provides new solutions as mentioned in Eq. 12.

$$stepsize_i = 0.01 \bullet \left(\frac{v_i}{u_i}\right) 1/\lambda \bullet \left(u - Y_{best}\right); \tag{12}$$

where $u \in \sigma_v randn[C]$ and $u \in randn[C]$. The random [C] signifies random scalar haggard from the average normal circulation. Then the new nest ν can be obtained by the subsequent calculation shown in Eq. 13:

$$u = u + stepsize_i \times randn[C]; \tag{13}$$

To enhance global research capability in relatively young generations, we propose further exploratory variations of the innovation strategy combining existing vectors and different vectors of random solutions. The new plan can be revealed in Eq. 14:

$$u = u + stepsize_i \times rand[C] + rand[C] \times \left(u - Y_{rand}\right); \tag{14}$$

In the next section, the Nest crossover function will be used to create new answers founded on the new explanation and the target vector. This process can be designated below Eq. 15:

$$\mathrm{u_j} = \begin{cases} Y_j + rand \times (Y_{R1} - Y_{R2}) & rand \le qb \\ Y_j & otherwise \end{cases} \tag{15}$$

Different types of strategies are suggested depending on the selected target vector and the figure of differential vectors used. The subsequent alteration techniques are often used in the nonfiction is given in Eq. 16:

$$u_j = Y_{R1} + f \times (Y_{R2} - Y_{R3}) \tag{16}$$

where R_1, R_2, $R_3 \in [1, ..., np]$ are arbitrarily produced different index satisfying $R_1 \neq R_2 \neq R_3 j$. F is the ascending factor.

$$\mathrm{u_{j,i}} = \begin{cases} Y_{R1,i} + rand \times (Y_{R2,i} - Y_{R3,i}) & rand \le qb \\ Y_{j,i} & otherwise \end{cases} \tag{17}$$

Here, we utilize the deep probability neural network (DPNN) to compute the optimal control value for solving various problems with the cuckoo search (CS) algorithm. Although CS-DPNN training is outside of open-vx, importing pre trained networks and enabling access to them is an important part of the open-vx process. The input vector y ∈ Y, the leading neural network, converts it into a solution through layers of units that connect between units—linear graphs or nonlinear non-linear activation functions [12], resulting in a representation in Eq. 18,

$$\mathcal{L}_\theta(x) = D_k o \sigma o D_{k-1} \ldots \ldots o \sigma o D_2 o \sigma o D_1(x) \tag{18}$$

The algorithm 2 describes the working function of CH selection using CS-DPNN technique.

Algorithm 2 CH selection using CS-DPNN algorithm

Input	: CH design metrics, vector y ∈ Y
Output	: CH
1	To optimizes CH selection metrics
2	Prepare parameters c,a, and p
3	Given training set$u = u + stepsize_i \times randn[C];$
4	Calculate initial fitness for CH selection $y_j(s+1) = y_j(s) + (R^2 \times h^* - y_j(s)) \times g_j$
5	End for
6	For each $1 \leqslant k \leqslant K$
7	if $u \in randn[C]$
8	Update optimal solution using activation function $\mathcal{L}_\theta(x) = D_k \; o \; \sigma \; o \; D_{k-1} \ldots\ldots \; o \; \sigma \; o \; D_2 \; o \; \sigma \; o \; D_1(x)$
9	Update the value of target vector $u_j = \begin{cases} Y_j + rand \times (Y_{R1} - Y_{R2}) & rand \leq qb \\ Y_j & otherwise \end{cases}$
10	End for$N = \sum_{K=1}^{K} (c_K + 1) c_{K+1}$
11	End

Here, ◦ refers to the arrangement of meanings. Popular choices with activation function σ in comprise sigmoid meaning, tan function and controlled CS-DPNN function as given in Eq. 19.

$$\sigma(w) = \max(w, 0) \tag{19}$$

when z∈R p for some p > 1, then the output of the CS-DPNN meaning in (2.10) is appraised element wise is mentioned in Eq. 20.

$$D_K(w_K) = Z_K w_K + a_K, for Z_K \in \mathbb{R}^{c_K \times c_{K+1}} W_K \in \mathbb{R}^{c_k}, a_K \in \mathbb{R}^{c_{K+1}} \tag{20}$$

For reliability of representation, we set d1 = d and dK + 1 = 1. Thus, in the jargon of machine knowledge, our CS-DPNN network contains of an input layer, an output layer and (k − 1) hidden layers for some $1 < k \in \mathbb{N}$. The k^{th} hidden layer (with c_{k+1} neurons) is assumed an input vector $W_K \in \mathbb{R}^{c_k}$ k and converts it first by an affine linear map D_K (20) and then by a CS-DPNN nonlinear beginning function as σ (19). A forthright calculation expression that our system comprises $\left(c + 1 + \sum_{K-1}^{K} c_K\right)$ neurons. We also denote,

$$\theta = \{Z_K, a_K\}, \theta_Z = \{Z_K\} \forall 1 \leq K \leq K, \tag{21}$$

$$N = \sum_{K=1}^{K} (c_K + 1) c_{K+1} \tag{22}$$

 https://doi.org/10.1007/s44196-025-00896-3

7 Optimal Route Computation Using Hybrid Recurrent Dynamic Neural Network (RDNN)

A session of synthetic neural networks where the connection between nodes forms a map, with or without a temporary array, is called a hybrid recurrent dynamic neural network. This enables it to display dynamic behaviour over time. Networks of both kinds display ephemeral dynamic activity. A variety of sensory data can be used by the hidden layers and traditional neural network layers to extract information. Furthermore, by merging data from several sensors, the particular method accomplishes sensor integration at the data level. The Recurrent Dynamic Neural Network (RDNN) contributes to reducing packet loss by enabling intelligent and adaptive routing decisions based on the temporal behavior and real-time status of the network. Unlike traditional routing approaches that rely on static metrics, RDNN leverages its recurrent architecture to maintain memory of past network conditions—such as node mobility patterns, link reliability, and congestion status—and uses this historical context to predict the most stable and efficient next-hop cluster head (CH) for data forwarding. By integrating both short-term and long-term dependencies through its hidden layers and gated mechanisms, RDNN ensures that routing decisions dynamically adapt to rapid topological changes, minimizing disruptions and link failures. This predictive capability reduces the likelihood of selecting unstable routes, thereby lowering the chances of data being dropped due to node disconnections or sudden mobility, which is particularly critical in mobile healthcare monitoring scenarios where real-time and reliable data transmission is essential.

The HR-DNN jobs are incompatible with the problem described in this broadsheet, although they can be handled more effectively than numerous inputs to multiple solutions. The circuit's input is a temporal sequence, each input value has a continuous link, and the seismic input from the previous instant inevitably disrupts the seismic response from the following instant. Additionally, there is obvious frenzy when tilt heights are accelerated, and story loss occurs. This function is an extension of the HR-DNN structure. The main purpose is that the construction of the HR-DNN permits material to be exchanged each time g_s as mentioned in Eq. 23

$$g_s^{(m)} = \sigma(Z_s^{(m)} \cdot \left[g_{s-1}^{(m)}, y_s^{(m)}\right] + V_s^{(m)} g_{s-1}^{(m)} + a_f^{(m)}) \tag{23}$$

The end nodes of simple HR-RNNs, however, have the drawback of being too weak to extract content from the period nodes at very large intervals. The hidden layer proposes that the gateway system can be used to control the stream and material loss to address the issue of long-term dependency. The primary components of the hidden layer are the input, output, and output ports. Values are expressed in the process of further transmission. The hidden layer is actually composed of two parts: one is multiplied by the gate of the admission of the newly obtained knowledge of this moment, and the other is multiplied by the long-term recall of the previous minute by the elapsed gate. They represented by the following Eqs. 24–29.

$$j_s^{(m)} = \sigma(Z_j^{(m)} \cdot \left[g_{s-1}^{(m)}, y_s^{(m)}\right] + a_j^{(m)}) \tag{24}$$

$$f_s^{(m)} = \sigma(Z_f^{(m)} \cdot \left[g_{s-1}^{(m)}, y_s^{(m)}\right] + a_f^{(m)}) \tag{25}$$

$$O_s^{(m)} = \sigma(Z_O^{(m)} \cdot \left[g_{s-1}^{(m)}, y_s^{(m)}\right] + a_O^{(m)}) \tag{26}$$

$$g_s^{(m)} = O_O^{(m)} \cdot \tan g\,(D_s) \tag{27}$$

$$\tilde{D}_s^{(m)} = \tan g\ (Z_d^{(m)} \cdot \left[g_{s-1}^{(m)}, y_s^{(m)}\right] + a_d^{(m)}) \tag{28}$$

$$D_s^{(m)} = f_s^{(m)} \cdot D_{s-1}^{(m)} + j_s^{(m)} \cdot \tilde{D}_s^{(m)} \tag{29}$$

Here, $j_s^{(m)}$), $f_s^{(m)}$, $O_O^{(m)}$ and $D_s^{(m)}$ are the response gate, elapsed gate, production gate and cell national unit of the s-th hidden layer at time s, correspondingly; $Z_j^{(m)}$, $Z_f^{(m)}$, $Z_O^{(m)}$ and $Z_d^{(m)}$ are all weight coefficient conditions; $a_j^{(m)}$, $a_f^{(m)}$, $a_O^{(m)}$ and $a_d^{(m)}$ are all bias trajectories.

Furthermore, a hidden layer alternative with fewer possibilities and quicker learning integration is the GRU layer. Figure 2 depicts the HR-DNN technique's construction. Update gates are utilised in place of GRU gates and input gates, and the deployment procedure is as follows in Eqs. 30–33.

$$R_s^{(m)} = \sigma(Z_R^{(m)} \cdot \left[g_{s-1}^{(m)}, y_s^{(m)}\right] + a_R^{(m)}) \tag{30}$$

$$W_s^{(m)} = \sigma(Z_W^{(m)} \cdot \left[g_{s-1}^{(m)}, y_s^{(m)}\right] + a_W^{(m)}) \tag{31}$$

$$\tilde{g}_s^{(m)} = \tan g(Z_g^{(m)} \cdot \left[R_s^{(m)} \cdot g_{s-1}^{(m)}, y_s^{(m)}\right] + a_g^{(m)}) \tag{32}$$

$$g_s^{(m)} = (1 - Z_s^{(m)}) \cdot \tilde{g}_s^{(m)} + W_s^{(m)} \cdot g_{s-1}^{(m)} \tag{33}$$

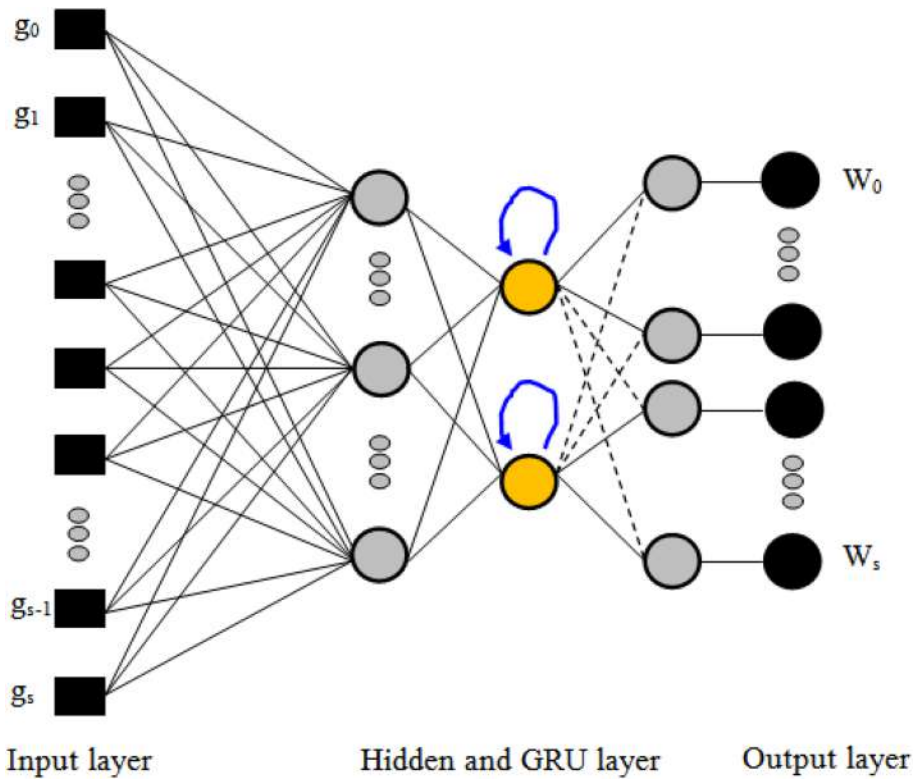

Fig. 2 Structure of our HR-DNN technique

Here, $Z_s^{(m)}$ and $R_s^{(m)}$ are, respectively, the nth GRU level's aware access and rearrange access at time s; $\tilde{g}_s^{(m)}$ is the applicant value; $g_{s-1}^{(m)}$ is the previous output value. It is important to note that it can aid in the memory of long-term time arrangement dependencies $R_s^{(m)}$ as well as the incarceration of short-term dependences $Z_s^{(m)}$. Algorithm 3 explains the working principle of the proposed HR-DNN method.

Algorithm 3 Route computation using HR-DNN

Input	: CH metrics
Output	: Select optimal neighboring CH node for routing
1	Initialize the values for the input parameters
2	Set a sample training as $g_s^{(m)} = \sigma(Z_s^{(m)} \cdot \left[g_{s-1}^{(m)}, y_s^{(m)}\right] + V_s^{(m)} g_{s-1}^{(m)} + a_f^{(m)})$
3	Compute hidden layer of network using $g_s^{(m)} = (1 - Z_s^{(m)}) \cdot \tilde{g}_s^{(m)} + W_s^{(m)} \cdot g_{s-1}^{(m)}$
4	Optimizes hidden layer using $R_s^{(m)} = \sigma(Z_R^{(m)} \cdot \left[g_{s-1}^{(m)}, y_s^{(m)}\right] + a_R^{(m)})$
5	End while
6	Optimize offset using $W_s^{(m)} = \sigma(Z_W^{(m)} \cdot \left[g_{s-1}^{(m)}, y_s^{(m)}\right] + a_W^{(m)})$
7	End

8 Results and Discussion

In this result slice, we evaluate and validate our proposed optimal cluster-based data loss aware routing protocol (OCDL-HM) in which the head node collects information from every other cluster node, carries out specific aggregation tasks, and then transmits the combined information to the base station through there different simulation scenarios. The simulations are conducted using NS3.26 simulator with the impact of nodes, node speed and imitation discs. NS3.26 is a traditional network test apparatus with several sensor nodes was employed for this testing. To increase the protocol's applicability, the base station is kept far from the target area.

9 Simulation Setup

Summary of our planned OCDL-HM routing protocol is summarized as follows: A butterfly induced sunflower optimization (BSFO) algorithm is used for cluster formation. The algorithm's design considers the unique behaviour of sunflowers to determine the optimal orientation with respect to the sun. By considering the minimum distance between flowers I and I + 1, the SFO algorithm simulates the pollination process through the random generation of seeds. The algorithm's primary goal is to stabilise plants near the sun and reduce the space between them so they can get sunlight. Then, the CH is computed through CS-DPNN. After that, the next neighbouring CH node is select by hybrid recurrent dynamic neural network (RDNN) which provides data lossless routing between nodes. In this simulation, we considered mobile-IoT nodes which placed randomly in the size of 1000×1000 m^2 network area. Nodes are detached by Euclidean distance between them. We chose the Wi-Fi802.11bprotocol and the CBR type traffic. We vary the number of IoT nodes as 50, 100, 150, 200 and 250 with the data transfer rate of 88Mbps. The initial transmission and getting power of sensor nodes are 1.4 W and 1.0 W. The original energy consumption of each node in network is 100 J. This statistics size of every mobile-IoT node is 512 bytes. The simulation results of proposed OCDL-HM routing protocol are associated with the present state-of-art routing protocols such as OLSR-SD, AQ-Routing and OLSR-ETX [33] in relations of energy consumption, packet

Table 2 Simulation Setup

Parameters	Values
Number of mobile IoT nodes	50, 100, 150, 200 and 250
Simulation time	100 s
Node initial energy	100 J
Node transfer power	1.4 W
Node receiving power	1.0W
Transmission range	250 m
MAC protocol	Wi-Fi802.11b
Traffic type	CBR
Node density	200–1000
Data size	88 Mbps
Node mobility (m/s)	5, 10, 15, 20 and 25
Mobility model	Random waypoint
Network size	800×600 m^2
Number of simulation rounds	10, 20, 30, 40 and 50

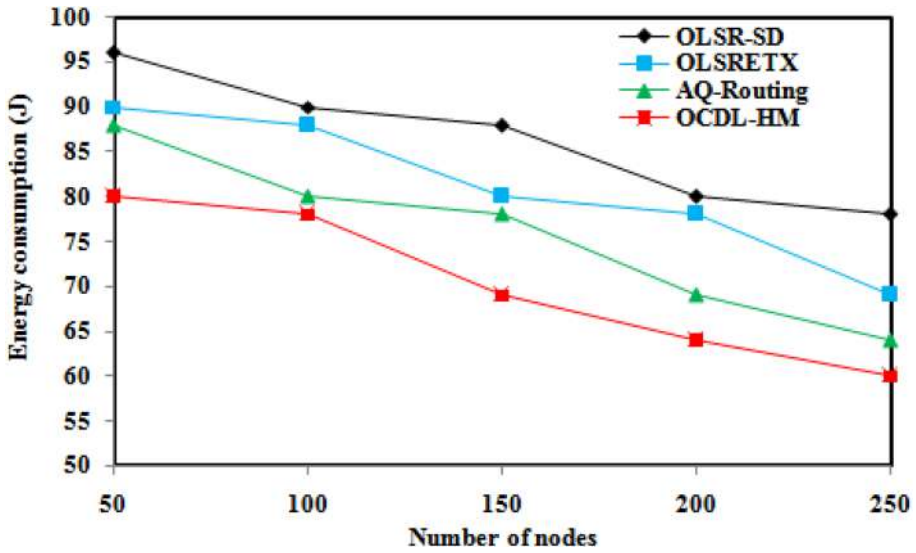

Fig. 3 Effect of energy consumption at the variable number of nodes scenario

delivery ratio, network lifetime, number of alive nodes, packet loss ratio, throughput and latency. The summary of simulation scenario is defined in Table 2.

10 Variable Number of Nodes

In this examination, we vary the quantity of mobile-IoT nodes as 50, 100, 150, 200 and 250 with the fixed node mobility as 20 m/s. Figures 3–9 shows the comparative analysis of proposed and existing state-of-art routing protocols. From the observed results of Fig. 3, the energy consumption of proposed OCDL-HM routing protocol is 23.08%, 17.95% and 11.54% lower than the existing state-of-art OLSR-SD, OLSR-ETX and AQ-Routing protocols. Energy consumption in MANET-IoT systems varies with node density primarily due to changes in communication overhead, routing complexity, and transmission distance among nodes. As node density increases, more nodes become available for forming clusters and relaying data, which can potentially reduce the average transmission distance between communicating nodes. This can lead to localized communication and lower energy expenditure per transmission. However, higher node density also results in increased

 https://doi.org/10.1007/s44196-025-00896-3

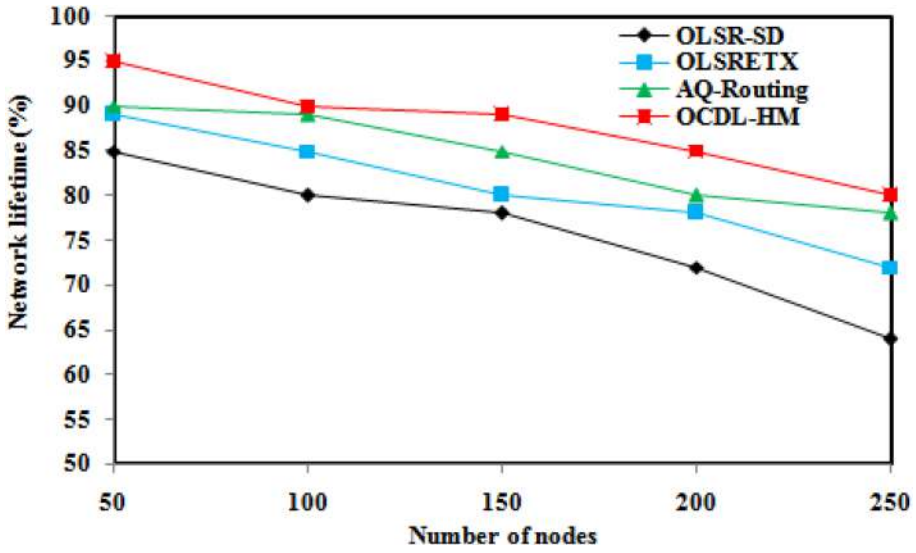

Fig. 4 Effect of network lifetime at the variable number of nodes scenario

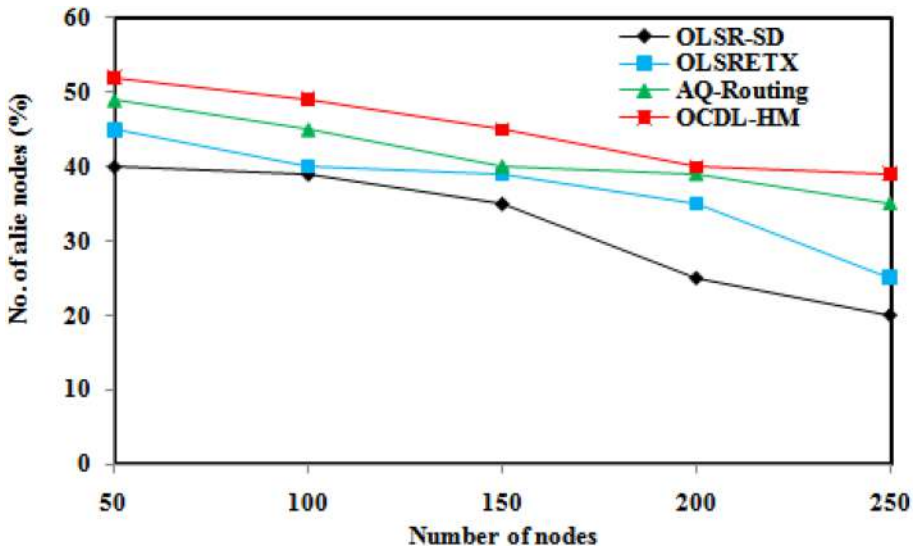

Fig. 5 Consequence of number of alive nodes at the variable number of nodes scenario

control message exchanges, frequent cluster reconfigurations, and a higher likelihood of data collisions and retransmissions, especially in mobile environments. These factors collectively increase the energy consumed by each node for maintaining network connectivity and ensuring reliable data transmission. Conversely, at very low densities, nodes may be farther apart, requiring higher transmission power to reach neighboring nodes, which again raises energy consumption. Therefore, the relationship between energy consumption and node density is nonlinear and depends on how efficiently the routing protocol adapts to these changing conditions. The proposed OCDL-HM protocol mitigates excessive energy drain by optimizing cluster formation and routing paths dynamically based on node availability and mobility, thereby maintaining energy efficiency across varying densities.

From the observed results of Fig. 4, the network lifetime of planned OCDL-HM routing protocol is 20.00%, 10.00% and 2.50% higher than the existing state-of-art OLSR-ETX and AQ-Routing protocols and OLSR SD.

From the observed results of Fig. 5, the quantity of active nodes of planned OCDL-HM routing protocol is 48.72%, 35.90% and 10.26% higher than the existing state-of-art OLSR-SD, OLSR-ETX and AQ-Routing protocols. From the observed results of Fig. 6, the packet delivery ratio of planned OCDL-HM routing protocol is 31.58%, 15.79% and 5.26% higher than the existing state-of-art OLSR-SD, OLSR-ETX and AQ-Routing

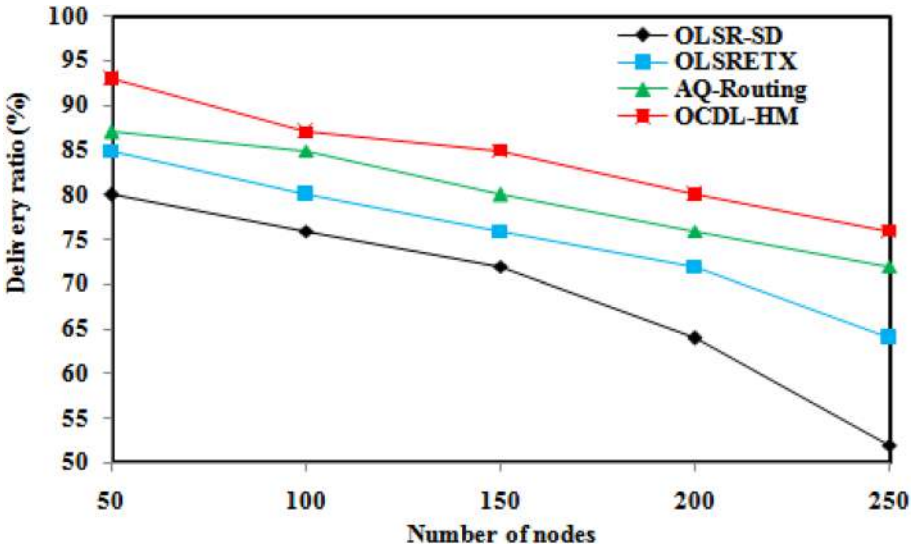

Fig. 6 Effect of packet delivery ratio at the variable number of nodes scenario

protocols. From the observed results of Fig. 7, the packet loss ratio of proposed OCDL-HM routing protocol is 44.12%, 40.63% and 32.14% lower than the existing state-of-art OLSR-ETX and AQ-Routing protocols and OLSR SD.

From the observed results of Fig. 8, the throughput of proposed OCDL-HM routing protocol is 12.50%, 7.50% and 5.00% higher than the existing state-of-art OLSR-SD, OLSR-ETX and AQ-Routing protocols. From the observed results of Fig. 9, the latency of proposed OCDL-HM routing protocol is 36.08%, 30.34% and 20.51% lower than the existing state-of-art OLSR-ETX and AQ-Routing protocols and OLSR SD.

11 Varying Node Speed

In this examination, we differ the speed of mobile-IoT nodes as 5, 10, 15, 20 and 25 m/s with the secure number of nodes as 250. Figures 10, 11, 12, 13, 14, 15, 16 show the comparative analysis of planned and existing state-of-art routing protocols. From the observed results of Fig. 10, the energy consumption of planned OCDL-HM routing protocol is 20.134%, 14.835% and 7.470% lower than the existing state-of-art OLSR-SD, OLSR-ETX

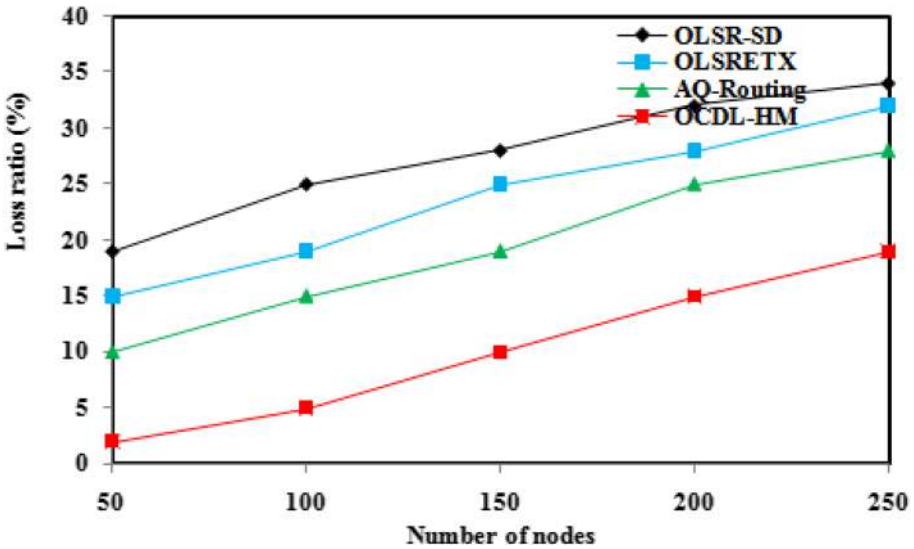

Fig. 7 Consequence of packet loss ratio at the variable number of nodes scenario

https://doi.org/10.1007/s44196-025-00896-3

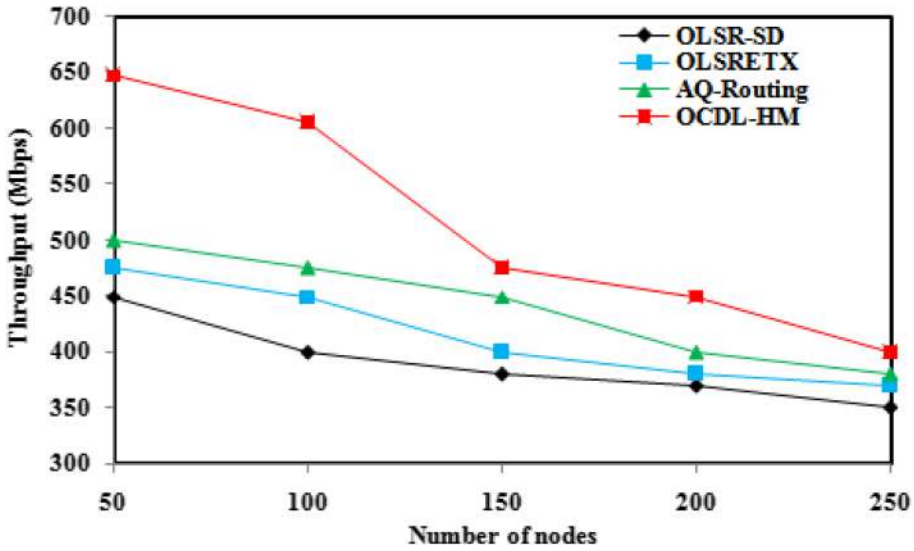

Fig. 8 Effect of throughput at the variable number of nodes scenario

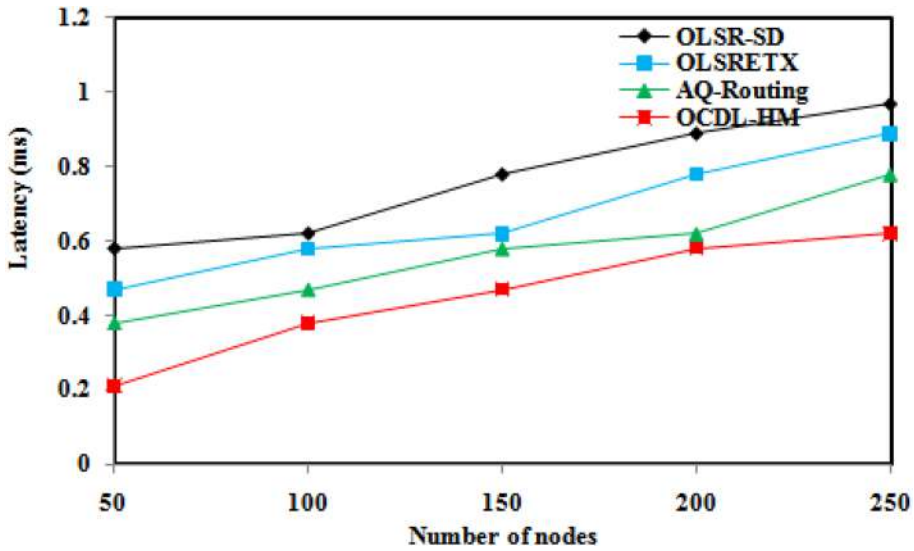

Fig. 9 Consequence of latency at the varying number of nodes scenario

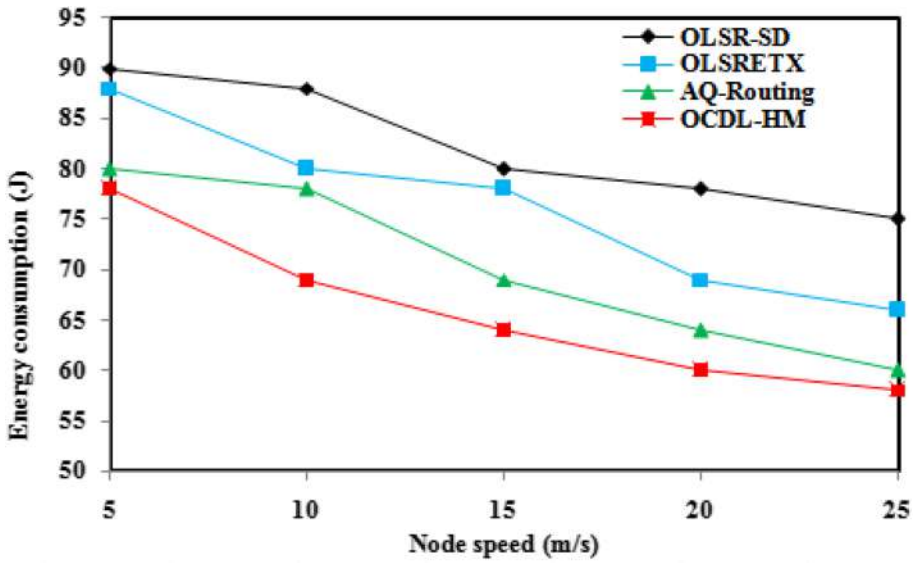

Fig. 10 Consequence of energy consumption at the varying number of nodes scenario

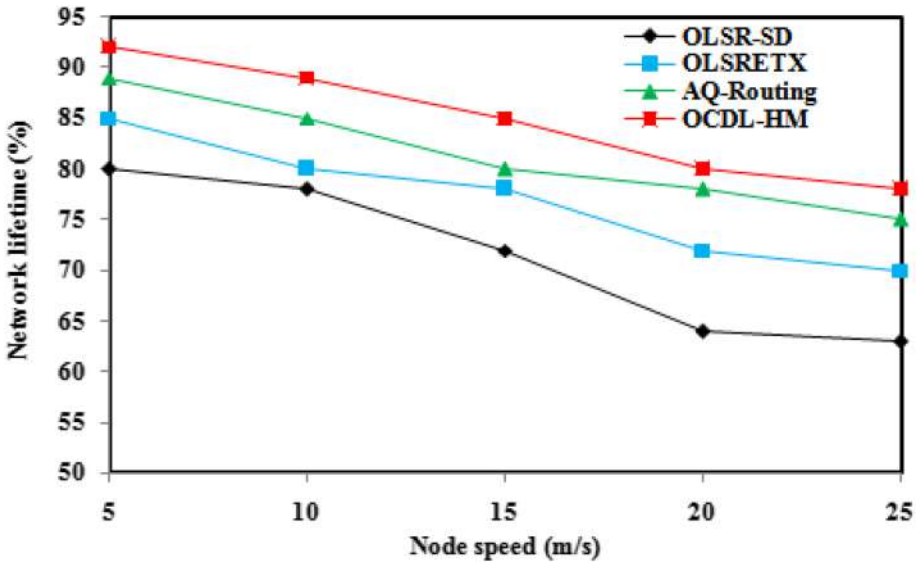

Fig. 11 Effect of network lifetime at the variable node speed

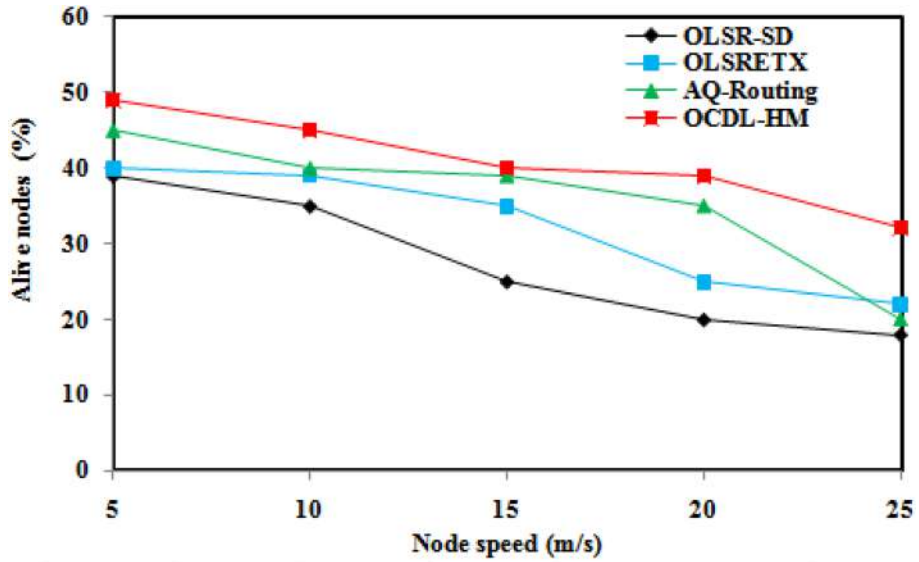

Fig. 12 Consequence of number of alive nodes at the variable node speed

and AQ-Routing protocols. From the observed results of Fig. 11, the network lifetime of proposed OCDL-HM routing protocol is 15.986%, 9.243% and 3.997% higher than the existing state-of-art OLSR-SD, OLSR-ETX and AQ-Routing protocols. From the observed results of Fig. 12, the quantity of active nodes of planned OCDL-HM routing protocol is 34.520%, 22.270% and 13.906% higher than the existing state-of-art OLSR-ETX and AQ-Routing protocols and OLSR SD.

From the observed results of Fig. 13, the packet delivery ratio of proposed OCDL-HM routing protocol is 22.390%, 12.669% and 4.770% higher than the existing state-of-art OLSR-SD, OLSR-ETX and AQ-Routing protocols. From the observed results of Fig. 14, the packet loss ratio of planned OCDL-HM routing protocol is 56.877%, 52.026% and 43.442% lower than the existing state-of-art OLSR-SD, OLSR-ETX and AQ-Routing protocols. From the observed results of Fig. 15, the throughput of proposed OCDL-HM routing protocol is 19.990%, 14.472% and 9.625% higher than the existing state-of-art OLSR-SD, OLSR-ETX and AQ-Routing protocols. From the observed results of Fig. 16, the latency of proposed OCDL-HM routing protocol is 36.840%, 28.059% and 14.306% lower than the existing state-of-art and OLSR-ETX and AQ-Routing protocols and OLSR SD.

 https://doi.org/10.1007/s44196-025-00896-3

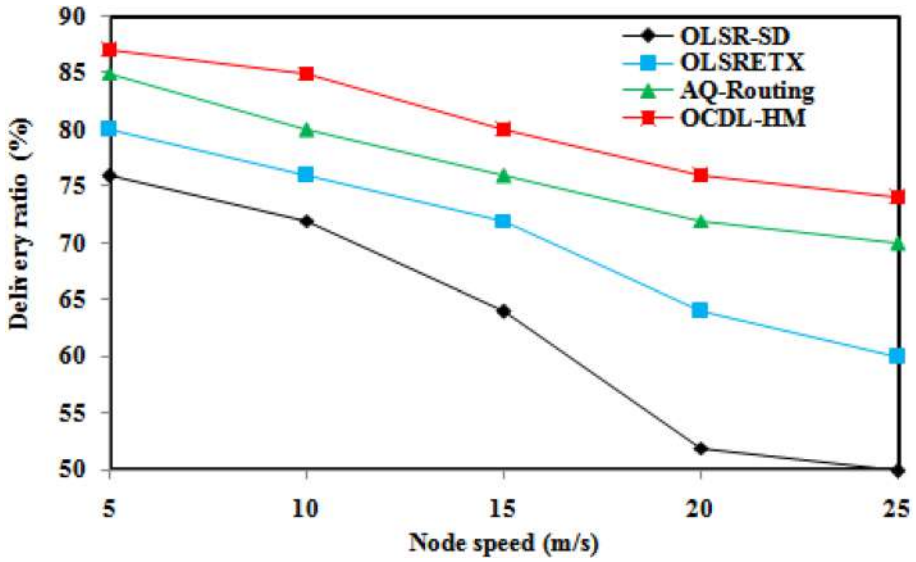

Fig. 13 Effect of packet delivery ratio at the variable node speed

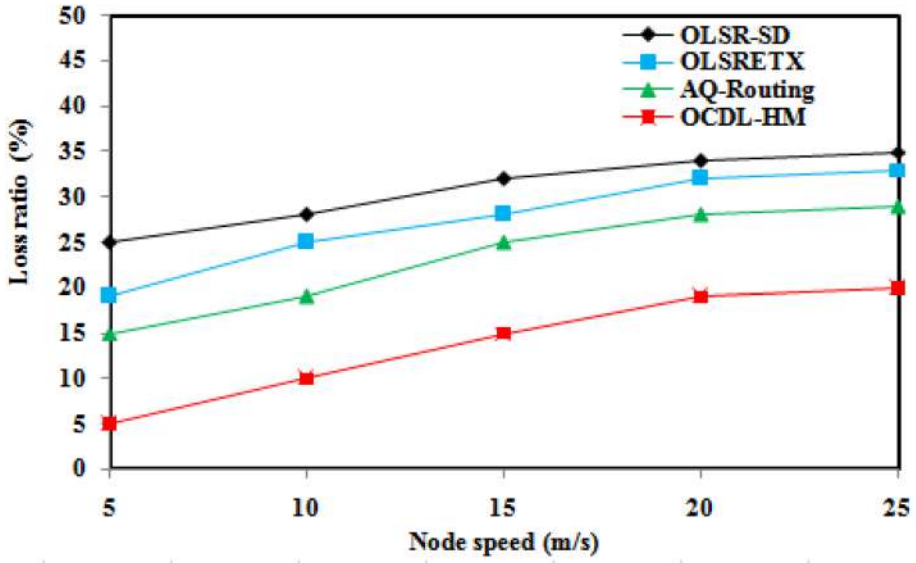

Fig. 14 Consequence of packet loss ratio at the variable knot speed

12 Variable Number of Simulation Series

In this assessment, we vary the simulation rounds as 10, 20, 30, 40 and 50 with the permanent quantity of knots as 250. Figures 17, 18, 19, 20, 21, 22, 23 show the comparative analysis of proposed and existing state-of-art routing protocols. From the observed results of Fig. 17, the energy consumption of proposed OCDL-HM routing protocol is 22.672%, 16.448% and 9.218% lower than the existing state-of-art OLSR-ETX and AQ-Routing protocols and OLSR-SD.

From the observed results of Fig. 18, the network lifetime of proposed OCDL-HM routing protocol is 17.587%, 9.826% and 4.134% higher than the existing state-of-art OLSR-SD, OLSR-ETX and AQ-Routing protocols. From the observed results of Fig. 19, the quantity of active nodes of planned OCDL-HM routing protocol is 39.771%, 25.263% and 14.482% higher than the existing state-of-art OLSR-SD, OLSR-ETX and AQ-Routing protocols. From the observed results of Fig. 20, the packet delivery ratio of proposed OCDL-HM

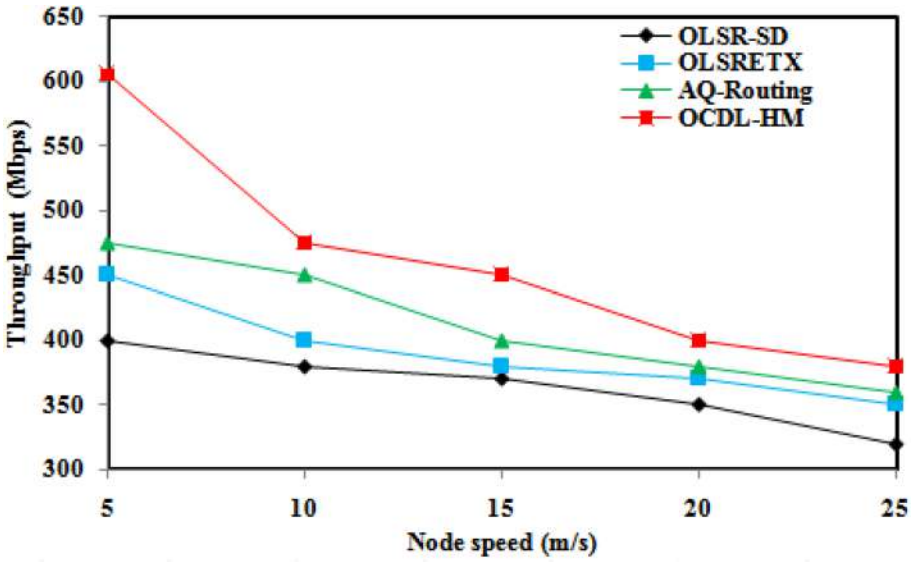

Fig. 15 Consequence of throughput at the variable knot speed

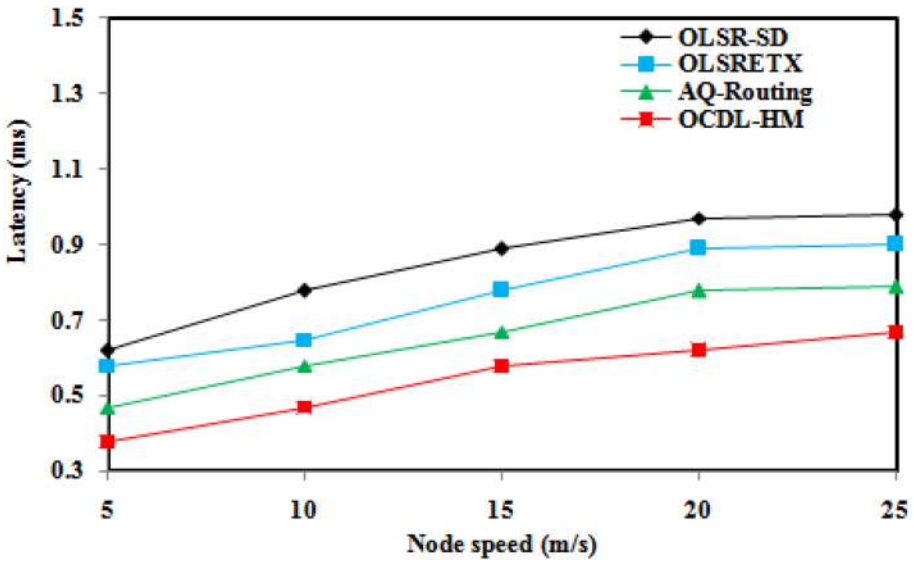

Fig. 16 Effect of latency at the varying node speed

routing protocol is 26.528%, 14.670% and 5.421% higher than the existing state-of-art OLSR-ETX, AQ-Routing protocols and OLSR-SD.

From the observed results of Fig. 21, the packet loss ratio of planned OCDL-HM routing protocol is 48.985%, 44.718% and 35.442% lower than the existing state-of-art OLSR-SD, OLSR-ETX and AQ-Routing protocols. From the observed results of Fig. 22, the throughput of proposed OCDL-HM routing protocol is 15.991%, 11.570% and 6.439% higher than the existing state-of-art OLSR-SD, OLSR-ETX and AQ-Routing protocols. From the observed results of Fig. 23, the latency of proposed OCDL-HM routing protocol is 35.921%, 26.229% and 11.810% lower than the existing state-of-art, OLSR-ETX, AQ-Routing protocols and OLSR-SD.

 https://doi.org/10.1007/s44196-025-00896-3

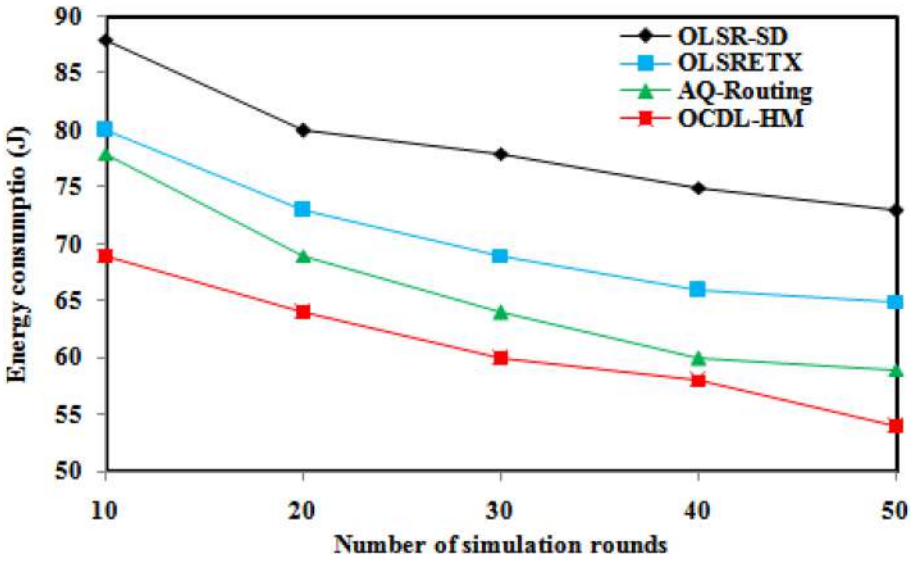

Fig. 17 Consequence of energy consumption at the variable number of nodes scenario

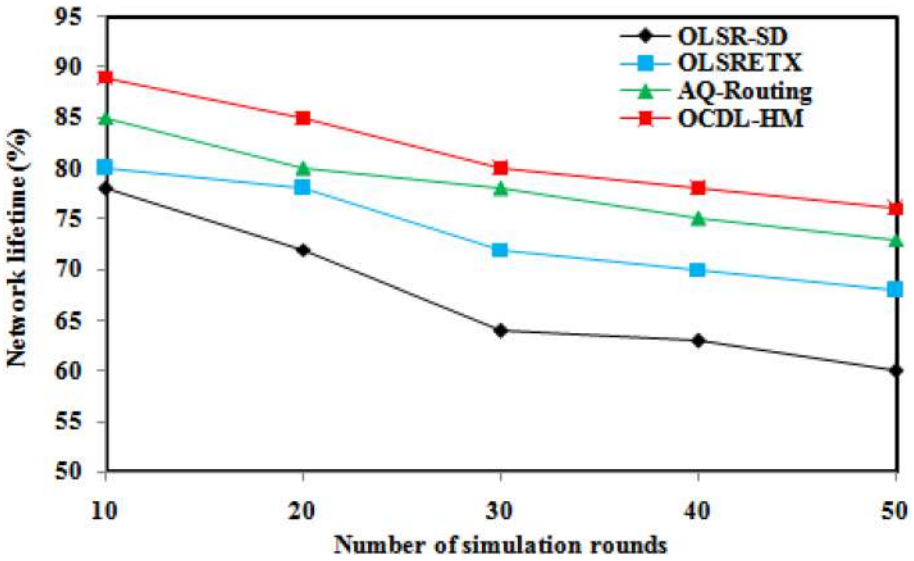

Fig. 18 Effect of network lifetime at the variable simulation rounds

13 Conclusion

The proposed OCDL-HM routing protocol demonstrates explicit improvements over existing routing protocols—namely OLSR-SD, OLSR-ETX, and AQ-Routing—through its multi-stage optimization and intelligent decision-making processes. Unlike conventional protocols that often suffer from packet loss, increased latency, and inefficient energy utilization due to static or less adaptive routing mechanisms, OCDL-HM employs a layered design integrating Butterfly-Induced Sunflower Optimization (BSFO) for energy-efficient cluster formation, Cuckoo Search-based Deep Probability Neural Network (CS-DPNN) for optimal cluster head selection, and Hybrid Recurrent Dynamic Neural Network (RDNN) for selecting the next best forwarding node. This design enables dynamic adaptation to topology changes, node mobility, and traffic conditions, significantly reducing data loss and improving routing reliability. Simulation results validate that the proposed protocol consistently outperforms existing models across multiple metrics, achieving lower energy consumption, higher packet delivery ratio, increased network lifetime, better throughput, and reduced latency, thereby offering a more robust and effective

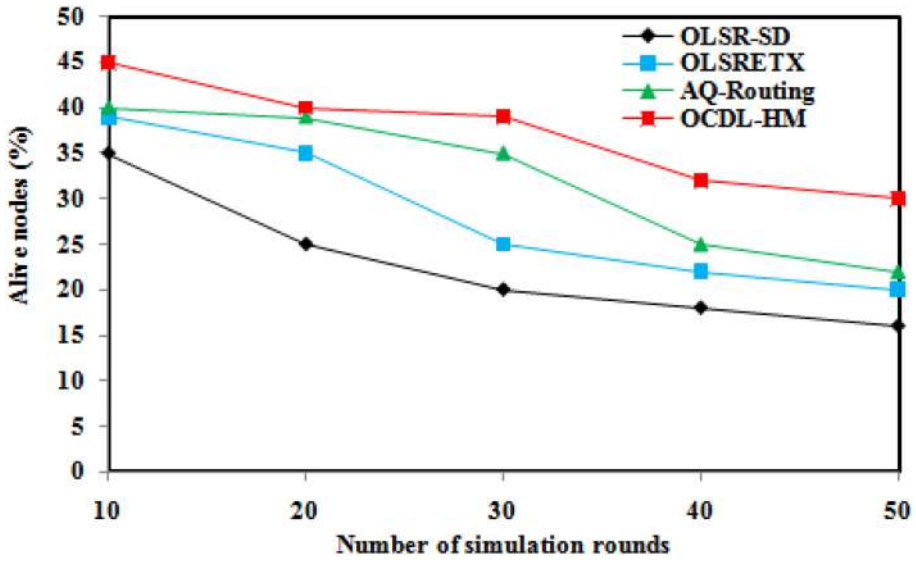

Fig. 19 Effect of number of alive nodes at the varying simulation rounds

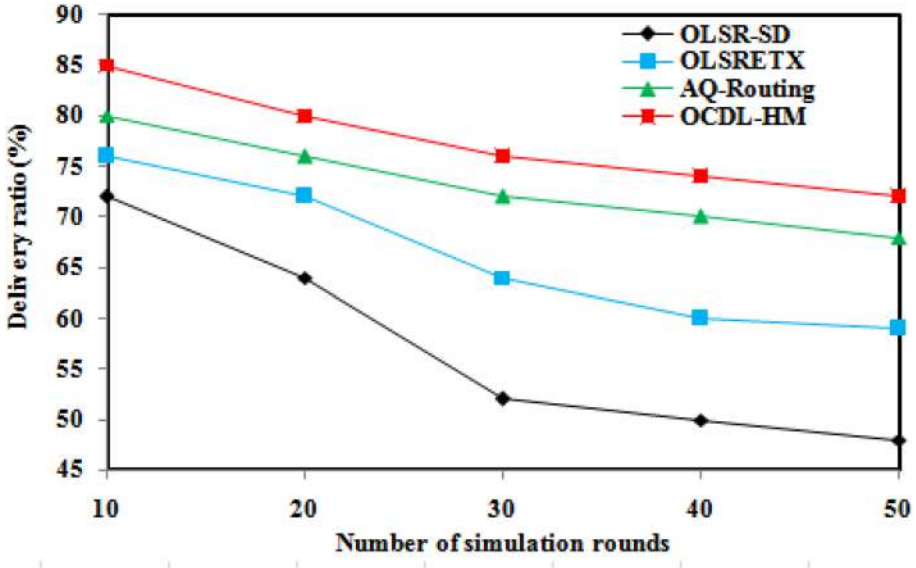

Fig. 20 Consequence of packet delivery ratio at the varying simulation rounds

solution for healthcare-focused MANET-IoT systems. We have proposed an optimal cluster-based data loss aware routing protocol MANET-IoT for healthcare monitoring system (OCDL-HM). An efficient cluster formation is done by butterfly induced sunflower optimization (BSFO) algorithm which enhances energy efficiency of routing. CH of each cluster is computed by cuckoo search based deep probability neural network (CS-DPNN) with the different design metrics. After that, the next neighbouring CH node is select by hybrid recurrent dynamic neural network (RDNN) which provides data lossless routing between nodes.

Since the reproduction outcomes, we observed that the effectiveness of planned OCDL-HM routing protocol is very high associated to the present state-of-art routing protocols. For variable number of nodes scenario, the performance planned OCDL-HM routing protocol is 12.585%, 8.584%, 18.886%, 11.428%, 60.306%, 18.083% and 32.863% efficient than the present routing protocols in positions of energy consumption, packet delivery ratio, network lifetime, quantity of active knots, packet loss ratio, throughput and latency respectively. For varying node speed scenario, the performance proposed OCDL-HM routing protocol is 14.146%, 9.742%, 23.565%, 13.276%, 50.782%, 14.696% and 26.402% efficient than the existing routing protocols in standings of energy

 https://doi.org/10.1007/s44196-025-00896-3

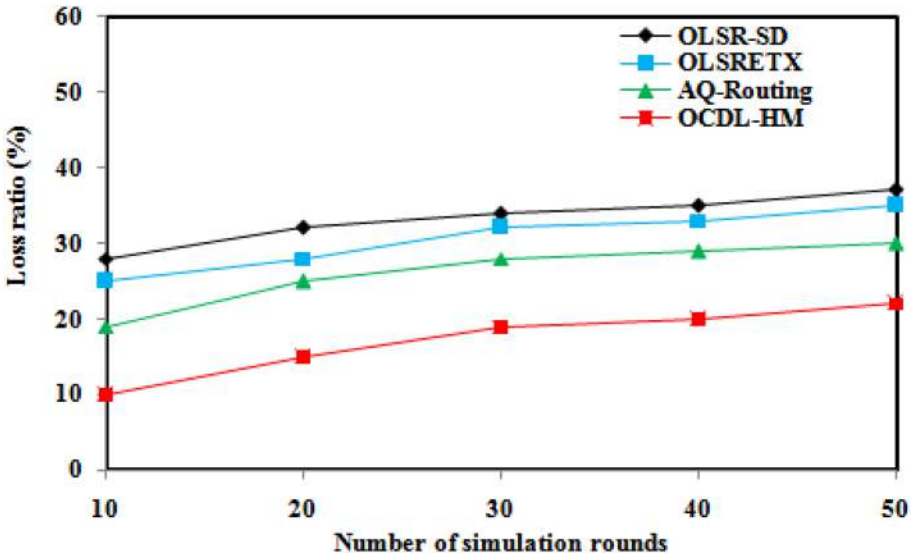

Fig. 21 Effect of packet loss ratio at the varying simulation rounds

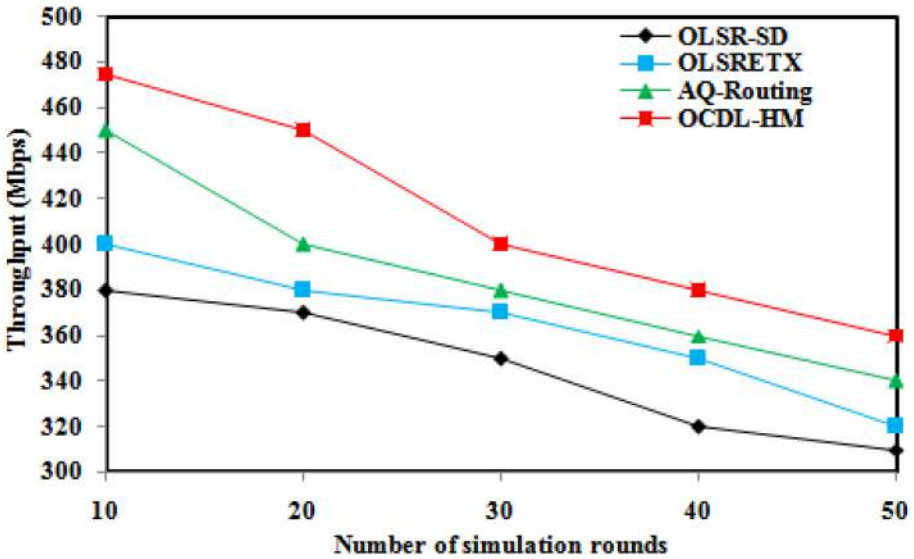

Fig. 22 Consequence of throughput at the varying simulation rounds

consumption, packet delivery ratio, network lifetime, quantity of active knots, packet loss ratio, throughput and latency respectively. For varying simulation rounds scenario, the performance proposed OCDL-HM routing protocol is 16.113%, 10.516%, 26.505%, 15.540%, 43.049%, 11.333% and 24.653% efficient than the present routing protocols in positions of energy consumption, packet delivery ratio, network lifetime, quantity of active knots, packet loss ratio, throughput and latency respectively.

While the proposed OCDL-HM routing protocol shows promising results in simulation, real-world implementation in healthcare environments may face several practical challenges. One significant hurdle is the variability in hardware capabilities among IoT devices, which can affect the consistent execution of complex algorithms like CS-DPNN and RDNN. Additionally, environmental factors such as signal interference in hospital settings, node failures, and mobility-induced disconnections can complicate reliable data transmission. Energy limitations in battery-operated medical devices may also restrict continuous operation, especially under high communication loads. Moreover, ensuring patient data privacy and compliance with healthcare

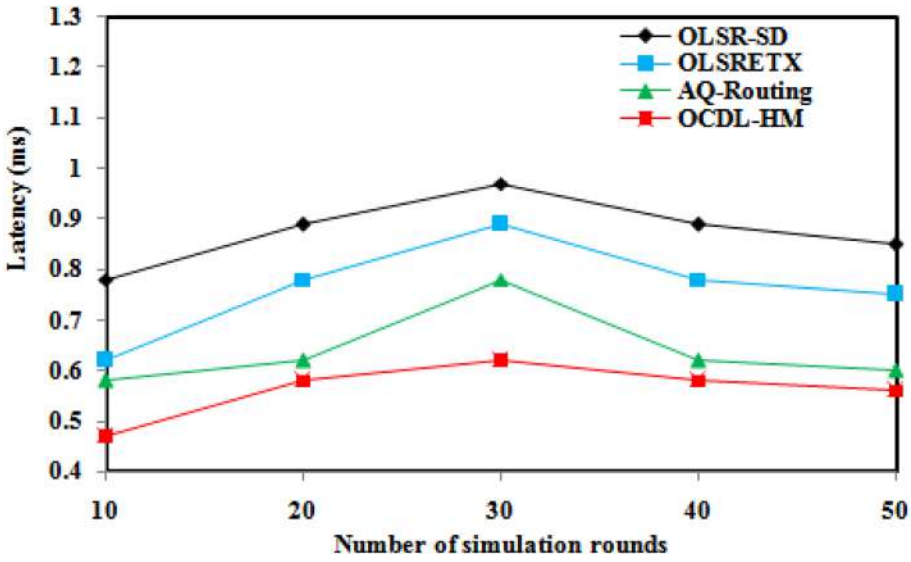

Fig. 23 Effect of latency at the varying simulation rounds

regulations, such as HIPAA or GDPR, introduces additional constraints on data handling and transmission. Future directions include developing lightweight versions of the proposed algorithms tailored for low-power embedded systems, integrating blockchain or secure edge computing for enhanced data security, and conducting field trials in controlled medical environments to validate performance. Enhancing interoperability with existing healthcare IT infrastructure and adapting the protocol to support hybrid cloud-edge architectures could further expand its applicability in smart healthcare systems.

Acknowledgements Not applicable.

Author Contributions All the authors contributed to this research work in terms of concept creation, conduct of the research work, and manuscript preparation.

Funding No funding was received for this research work.

Data Availability The datasets used and/or analyzed during the current study are available from the corresponding author upon reasonable request.

Declarations

Conflict of interest The authors declare no competing interests.

Ethics Approval and Consent to Participate Not applicable.

Consent for Publication Not applicable.

References

1. Serhani, A., Naja, N., Jamali, A.: AQ-Routing: mobility-, stability-aware adaptive routing protocol for data routing in MANET–IoT systems. Clust. Comput.. Comput. **23**(1), 13–27 (2020)
2. Tan, S., Li, X., Dong, Q.: Trust based routing mechanism for securing OSLR-based MANET. Ad Hoc Netw.Netw. **30**, 84–98 (2015)
3. Ismail, N.H.A., Hassan, R.: 6LoWPAN local repair using bio inspired artificial bee colony routing protocol. Procedia Technol. **11**, 281–287 (2013)
4. Miao, Y., et al.: Time-controllable keyword search scheme with efficient revocation in mobile E-Health cloud. IEEE Trans. Mob. Comput.Comput. **23**(5), 3650–3665 (2024). https://doi.org/10.1109/TMC.2023.3277702
5. Yamarthy, M.R., Subramanyam, M.V., Prasad, K.S.: A multi-layer routing protocol for mobility management in wireless mesh networks. Procedia Comput Sci **89**, 51–56 (2016)
6. Guo, J., et al.: ICRA: an intelligent clustering routing approach for UAV Ad Hoc Networks. IEEE Trans. Intell. Transp. Syst.Intell. Transp. Syst. **24**(2), 2447–2460 (2023). https://doi.org/10.1109/TITS.2022.3145857
7. Yang T. et. al.: Secure and traceable multikey image retrieval in cloud-assisted internet of things. IEEE Internet Things J **11**, 40875–40887 (2024) https://doi.org/10.1109/JIOT.2024.3457017.
8. Ardakani, S.P., Padget, J., De Vos, M.: CBA: A cluster-based client/server data aggregation routing protocol. Ad Hoc Netw.Netw. **50**, 68–87 (2016)
9. Aydogdu, C., Sancakli, S.: Joint effect of data rate and routing strategy on energy-efficiency of IEEE 802.11 DCF based multi-hop wireless networks under hidden terminal existence. Ad Hoc Netw.Netw. **30**, 1–21 (2015)
10. Conti, M., Boldrini, C., Kanhere, S.S., Mingozzi, E., Pagani, E., Ruiz, P.M., Younis, M.: From MANET to people-centric networking: Milestones and open research challenges. Comput. Commun.. Commun. **71**, 1–21 (2015)
11. Rhaiem, O.B., Fourati, L.C., Ajib, W.: Network coding-based approach for efficient video streaming over MANET. Comput. Netw.. Netw. **103**, 84–100 (2016)
12. Narayandas, V., Dugyala, R., Tiruvayipati, S. and Yellasiri, R.: November. Necessity of MANET implementation over Internet of Things: The Future of Dynamic Communication among End Devices. In *2019 Fifth International Conference on Image Information Processing (ICIIP)* (pp. 359–362). IEEE (2019).
13. Karlsson, J., Dooley, L.S., Pulkkis, G.: August. Secure routing for MANET connected Internet of Things systems. In 2018 IEEE 6th international conference on future internet of things and cloud (FiCloud) (pp. 114–119). IEEE. (2018)
14. Schweitzer, N., Stulman, A., Margalit, R.D., Shabtai, A.: Contradiction based gray-hole attack minimization for ad-hoc networks. IEEE Trans. Mob. Comput.Comput. **16**(8), 2174–2183 (2016)
15. Anil, G.N.: Multi-level Trust Modelling to Resist Impact of Routing Attacks on Reliable Data/Communication Transactions in MANET-IoT Ecosystem. In *Computer Science On-line Conference* (pp. 196–205). Springer, Cham. (2021)
16. Al-Qarni, B.H., Almogren, A., Hassan, M.M.: An efficient networking protocol for internet of things to handle multimedia big data. Multimedia Tools Appl **78**(21), 30039–30056 (2019)
17. Kumar, A.,. Sharma, D.K.. An optimized multilayer outlier detection for internet of things (IoT) network as industry 4.0 automation and data exchange. In *International Conference on Innovative Computing and Communications* (pp. 571–584). Springer, Singapore. (2021)
18. Manivannan, R., Senthilkumar S., Senthil Kumar, T.: Improved restricted boltzmann machine-based optimization model for the network security system in cloud environment. *Eng. Res. Exp.*, **6**(2), 025313 (2024). https://doi.org/10.1088/2631-8695/ad3f77.
19. Trivedi, R., Khanpara, P.: Robust and secure routing protocols for MANET-based internet of things systems—A survey. In Emergence of Cyber Physical System and IoT in Smart Automation and Robotics (pp. 175–188). Springer, Cham (2021)
20. Gautam, A., Mahajan, R. and Zafar, S.: QoS Optimization in Internet of Medical Things for Sustainable Management. In Cognitive Internet of Medical Things for Smart Healthcare (pp. 163–179). Springer, Cham. (2021)
21. Vu, K.Q., Solanki, V.K. and Le, A.N., 2022. A Saving Energy MANET Routing Protocol in 5G. In *Secure Communication for 5G and IoT Networks* (pp. 213–220). Springer, Cham.
22. Kumar, A., Aggarwal, A.: December. An Efficient Outlier Detection Mechanism for RFID-Sensor Integrated MANET. In *International Conference on Intelligent Systems Design and Applications* (pp. 853–863). Springer, Cham. (2018)
23. Hemalatha, R., Umamaheswari, R., Jothi, S.: Optimal route maintenance based on adaptive equilibrium optimization and GTA based route discovery model in MANET. *Peer-to-Peer Netw. Appl.* **14**, 3416–3430 (2021)
24. Gupta, S., Snigdh, I.: Analyzing Impacts of Energy Dissipation on Scalable IoT Architectures for Smart Grid Applications. In *Advances in Smart Grid Automation and Industry 4.0* (pp. 81–89). Springer, Singapore. (2021)
25. Kang, D., Kim, H.S., Joo, C., Bahk, S.: ORGMA: Reliable opportunistic routing with gradient forwarding for MANETs. Comput. Netw.. Netw. **131**, 52–64 (2018)
26. Karmel, A., Vijayakumar, V., Kapilan, R.: Ant-based efficient energy and balanced load routing approach for optimal path convergence in MANET. Wireless Netw.Netw. **27**(8), 5553–5565 (2021)

27. da Costa Bento, C.R., Wille, E.C.G.: Bio-inspired routing algorithm for MANETs based on fungi networks. Ad Hoc Netw.Netw. **107**, 102248 (2020)
28. Hammi, B., Zeadally, S., Labiod, H., Khatoun, R., Begriche, Y., Khoukhi, L.: A secure multipath reactive protocol for routing in IoT and HANETs. Ad Hoc Netw.Netw. **103**, 102118 (2020)
29. Garg, M., Gupta, A., Kaushik, D., Verma, A.: Applying machine learning in IoT to build intelligent system for packet routing system. *Mater Today: Proc*. (2020)
30. Senthilkumar, T, Mohan, V., Senthilkumar, S.: Energy efficient transmission using optical access network: issues and challenges. Int. J. Eng. Sci. Technol., 7(1), 43–51 (2023). https://doi.org/10.29121/IJOEST.v7.i1.2023.462.
31. Djedjig, N., Tandjaoui, D., Medjek, F., Romdhani, I.: Trust-aware and cooperative routing protocol for IoT security. J Informat Security Appl **52**, 102467 (2020)
32. Niu, Z., Li, Q., Ma, C., Li, H., Shan, H., Yang, F.: Identification of critical nodes for enhanced network defense in MANET-IoT networks. IEEE Access **8**, 183571–183582 (2020)
33. Maruthupandi, J., Prasanna, S., Jayalakshmi, P., Mareeswari, V., Sanjeevi, P.: Route manipulation aware Software-Defined Networks for effective routing in SDN controlled MANET by Disney Routing Protocol. Microprocess. Microsyst.. Microsyst. **80**, 103401 (2021)
34. Simpson, S.V., Nagarajan, G.: A fuzzy based Co-Operative Blackmailing Attack detection scheme for Edge Computing nodes in MANET-IOT environment. Futur. Gener. Comput. Syst.. Gener. Comput. Syst. **125**, 544–563 (2021)
35. Wu, D., Li, H., Li, X., Zhang, J.: A geographic routing protocol based on trunk line in VANETs. In *Cyberspace Data and Intelligence, and Cyber-Living, Syndrome, and Health* (pp. 21–37). Springer, Singapore. (2019)
36. Arora, S., Singh, S.: Butterfly optimization algorithm: A novel approach for global optimization. Soft. Comput.Comput. **23**, 715–734 (2019)
37. Makhadmeh, S.N., Al-Betar, M.A., Abasi, A.K., et al.: Recent advances in butterfly optimization algorithm, its versions and applications. Arch Computat Methods Eng **30**, 1399–1420 (2023). https://doi.org/10.1007/s11831-022-09843-3
38. Wang, Y., Dai, S., Liu, P., Zhao, X.: A hybrid particle swarm optimization with butterfly optimization algorithm based maximum power point tracking for photovoltaic array under partial shading conditions. Sustainability **15**, 12402 (2023). https://doi.org/10.3390/su151612402
39. Yasin, S., Iqbal, N., Ali, T. et al.: Severity grading and early retinopathy lesion detection through hybrid inception-ResNet architecture. Sensors 20(21), 6933 (2021) https://doi.org/10.3390/s21206933
40. Hussain, A., Ali, T., Althobiani, F. et al. Security framework for IoT based real-time health applications. Electronics 10(6), 719 (2021) https://doi.org/10.3390/electronics10060719
41. Ali, T., Masood, K., Irfan, M. et al.: Multistage segmentation of prostate cancer tissues using sample entropy texture analysis. Entropy 22(12), 1370 (2020). https://doi.org/10.3390/e22121370
42. Khalid, M.J., Irfan, M., Ali, T., et al.: Integration of discrete wavelet transform, DBSCAN and classifiers for efficient content based image retrieval. Electronics (2020). https://doi.org/10.3390/electronics9111886
43. Ali, G., et al.: Artificial neural network based ensemble approach for multicultural facial expressions analysis. IEEE Access **8**, 134950–134963 (2020). https://doi.org/10.1109/ACCESS.2020.3009908
44. Ali, T., Noureen, J., Draz, U., Shaf, A., Yasin, S., Ayaz, M. Participants ranking algorithm for crowdsensing in mobile communication. EAI Endorsed Transactions on Scalable Information Systems. https://doi.org/10.4108/eai.13-4-2018.154476

Authors and Affiliations

K. Balasubramanian[1] · S. Senthilkumar[2] · N. Kopperundevi[3] · S. Sivakumar[4]

✉ K. Balasubramanian
kbala0211@gmail.com

✉ S. Senthilkumar
senthil.lanthiri@gmail.com

✉ N. Kopperundevi
kopperundevi.n@vit.ac.in

 https://doi.org/10.1007/s44196-025-00896-3

S. Sivakumar
sivakumarsathasivampillai@gmail.com

[1] Department of Information Technology, E.G.S. Pillay Engineering College, Nagapattinam 611002, Tamil Nadu, India

[2] Department of Electronics and Communication Engineering, E.G.S. Pillay Engineering College, Nagapattinam 611002, Tamil Nadu, India

[3] School of Computer Science and Engineering, Vellore Institute of Technology, Vellore 632014, Tamil Nadu, India

[4] Department of Computer Science and Engineering, Nehru Institute of Engineering and Technology, Coimbatore 641105, Tamil Nadu, India